# First-principles study of group III impurity doped PbSe: Bulk and nanowire

E. O. Wrasse and R. J. Baierle*
*Departamento de Física, Universidade Federal de Santa Maria, 97105-900, Santa Maria, RS, Brazil*

A. Fazzio
*Instituto de Física, Universidade de São Paulo, C.P. 66318, 05315–970, São Paulo, SP Brazil*

T. M. Schmidt
*Instituto de Física, Universidade Federal de Uberlândia, C.P. 593, 38400-902, Uberlândia, MG, Brazil*
(Received 30 August 2012; revised manuscript received 17 December 2012; published 19 February 2013)

Fully relativistic calculations are used to perform a systematic study on the energetic stability, and electronic properties of group III (Al, Ga, In, and Tl) impurities in the cation-site (Pb) of PbSe: bulk and nanowire (NW). Our results show that group III impurities have lower formation energies in the NW than in the bulk. The impurities are site-dependent in the nanowires: they are more stable on the surface of the NW as compared to the core. In the bulk, Al and In are donor levels, while Ga and Tl are acceptor impurities. For the NW, the same trend is obtained for Al and Tl, whereas Ga and In are deep donors. A two-level model based on the interaction between the impurity states and the host crystalline field explains the electronic properties of group III impurity doped PbSe bulk and NW. This model agrees with the projected density of states and helps us to understand the unexpected $n$-type character of some group III impurity doped PbSe.

DOI: 10.1103/PhysRevB.87.085428 PACS number(s): 71.15.Nc, 73.20.At, 73.22.−f

## I. INTRODUCTION

Lead chalcogenides like PbTe and PbSe semiconductor materials have the potential to be used in infrared lasers, diodes, detectors,[1–3] and spintronics[4,5] and are of especial interest for thermoelectric (TE) devices.[6,7] These narrow band gap semiconductors present strong spin-orbit (SO) effects that rule the energy position and dispersion of the states in the conduction band minimum (CBM), that comes mainly from the $6p$ orbitals of the Pb atoms.[8] Recently, we show that, in a nanoscale form, the SO coupling is even more important than in the bulk, determining not only the character of the band structure, but also the energy band gap.[9] Experimentally, it has been verified that nanostructured materials present better TE efficiency as compared to the bulk ones,[10–12] making nanostructured lead chalcogenides promising materials for TE applications.

PbTe has been largely studied as a promising TE material, either doped,[2,13–15] or derivative alloys based on PbTe,[16–21] and more recently in nanoscale form.[22] Although PbSe has been less studied than PbTe, the former present smaller thermal conductivity, that can improve the figure-of-merit ($ZT$).[23] Both PbTe and PbSe doped by group III elements (Ga, In, and Tl) have been studied since a long time and many models for the electronic properties have been proposed.[24] These models are helpful to understand important experimental observations, but first-principles calculations brought new insights that elucidated the fundamental physics on these doped materials.[13] An important insight in TE applications is the recent report by Zhang *et al.*[25] for Al doped PbSe. They obtained a huge increase in the $ZT$ for Al doped PbSe as compared to the undoped system, in which, based on a first-principles calculation, they attribute the higher $ZT$ to the increase in the electronic density of state (DOS) near the Fermi energy.

For an intrinsic semiconductor, the electronic structure and transport properties depend on the Fermi level position, which can run from the top of the valence band to the bottom of the conduction band, depending on whether it is a $p$- or an $n$-type semiconductor, respectively. For a doped semiconductor, when a sharp electronic level appears inside or near the band gap region, an increase in the electronic density of states in this region is observed. For transport properties, the DOS near the Fermi energy, the density of carriers (electrons and holes), the effective mass of the carriers, and the position of the electronic defective state are of fundamental importance. Those properties depend on the host semiconductor and the dopant. For a NW, due to the electronic quantum confinement perpendicular to the growth direction, we also have to consider that the band gap opens up, and the energy dispersions are different than those of the bulk.

In this work, we investigate the structural and electronic properties of group III impurity (Al, Ga, In, and Tl) doped PbSe bulk and NWs. Our *ab initio* results show that, not only Al impurity presents the unexpected $n$-type character, as observed experimentally by Zhang *et al.* in bulk PbSe,[25] but also In impurity induces $n$-type doping. For PbSe NWs, due to quantum confinement effects, the group III impurities induce $n$-type (Al), deep donor states (Ga and In), and also $p$-type doping (Tl). To explain the electronic properties for the doped system, we construct a two-level model based on the splitting of the impurity states in the presence of the crystalline field.[26] When impurities interact strongly with $p$ orbitals of the Se atoms, a $n$-type character is present, while those that present weaker interactions, result in a $p$-type system. We also observe that the interaction between the impurity states and the crystalline field changes from the bulk to the NW, which explains the different semiconductor characters observed in the low-dimensional system (NW).

## II. METHODOLOGY

The calculations are performed in the framework of the density functional theory (DFT) with the generalized gradient approximation (GGA)[27] for the exchange–correlation term.

 

The Kohn–Sham (KS) equations are solved using the self-consistent method, as implemented in the Vienna *ab initio* simulation package (VASP).[28,29] The valence electrons and the ionic core interactions are described through the PAW method.[30] The KS orbitals are expanded in a plane-wave basis set with an energy cutoff of 450 eV. In the calculations, the relativistic effects are properly treated by including the SO interactions.

Bulk PbSe crystallizes in the rock salt (RS) structure, which can be described using a face-centered cubic (fcc) unit cell with two atoms (Pb and Se) localized in the (0,0,0) and ($\frac{1}{2}$, $\frac{1}{2}$, $\frac{1}{2}$) positions, respectively. The experimental lattice parameter is $a_0 = 6.124$ Å and the direct band gap at the $L$ point is 0.17 eV at 300 K. Using the basic unit cell, we obtain a lattice equilibrium parameter of $a_0 = 6.200$ Å and a direct band gap of 0.30 eV at the $L$ point for standard DFT calculations (without SO). By adding the SO interactions, we obtain a band gap of 0.02 eV. The VBM is mainly composed by the $4p$ orbitals from Se atoms, while the CBM is mainly ruled by the $6p$ orbital from the Pb atoms. Our calculations are in agreement with results presented in the literature.[8,31]

When the impurities are incorporated, we use a supercell in order to minimize the nonrealistic effects due to the "periodic" doping. The supercell used is a simple cubic (sc) [(2×2×2)] with 64 atoms ($Pb_{31}X_1Se_{32}$). With this enlarged supercell, the fundamental band gap of the undoped bulk PbSe now is mapped at the Γ point, and due to the folder band, both CBM and VBM are fourfold (disregarding spins) degenerated.

To describe the PbSe NW system, we use a NW in the RS structure, aligned along the [001] direction. The NW preserves the 1 : 1 in-plane stoichiometry and has a diameter of 2.3 nm. For this NW, the equilibrium lattice parameter along the [001] direction is $c_0 = 6.178$ Å. To ensure negligible interactions between the wire images, a vacuum region of about 10.0 Å perpendicular to the wire axis is used (see Fig. 1). Similar to the bulk, the effects of nonrealistic periodic doping are minimized by using a supercell. The supercell has a length of $2c_0$ along the [001] direction, as depicted in Fig. 1.

In our calculations for doped PbSe (bulk and NW), all atoms in the enlarged supercell are allowed to relax, without imposing any symmetry constraint. The forces are calculated using the Hellmann-Feymann procedure and the geometries are optimized using the conjugated gradient (CG) method. The system is relaxed until the root mean square criterion of 0.04 eV/Å of the atomic forces is reached. To sample the Brillouin zone (BZ) and calculate the periodic functions, we use the procedure of the special $\vec{k}$ points described by Monkhorst and Pack.[32] To generate the special $\vec{k}$ points, a grid of 4×4×4 and 1×1×4 are used for the bulk and NW, respectively.

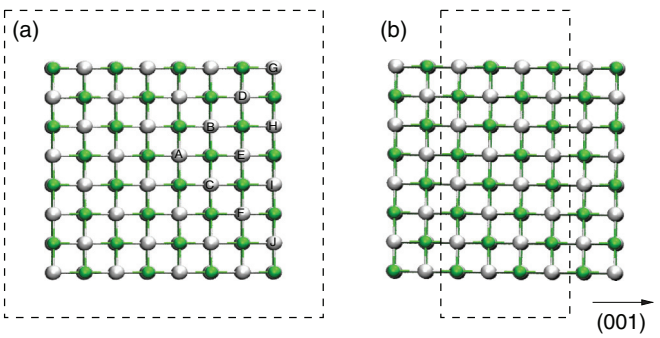


FIG. 1. (Color online) Cross-section (a) and lateral (b) views of the PbSe NW (2.3 nm in diameter) in the RS structure and aligned along the [001] direction. Small green spheres represent Se atoms and large gray spheres represent Pb atoms. The labels A to J indicate the sites where the impurities will be incorporated.

The formation energy $[E^f(X_{Pb})]$ of an impurity $X$ at the neutral ($q = 0$) charge state substituted at the cation (Pb) site can be written as

$$E^f(X_{Pb}) = E^T(X_{Pb}) - E^T(0) - \mu_{Pb} + \mu_X, \qquad (1)$$

where $E^T(X_{Pb})$ and $E^T(0)$ are the total energies of the supercell with a $X$ impurity and the undoped system, respectively. The atomic chemical potentials $\mu_{Pb}$ and $\mu_X$ ($X$ = Al, Ga, In, and Tl) are obtained as the total energy per atom of the most stable configuration: the metallic phase of each element. Negative value of $E^f(X_{Pb})$ indicates that the impurity is readily incorporated (an exothermic process).

## III. STRUCTURAL PROPERTIES

The optimized structure for group III impurities ($X$ = Al, Ga, In, and Tl) in Pb site of bulk PbSe, $X_{Pb}$, induce relaxations of the Se first neighbors of the impurity. The relaxations are proportional to the covalent radius of the impurities. The greater is the difference between the $X$ impurity and the Pb covalent radius, the greater is the structural relaxation. Following Eq. (1), we compute the formation energies for these impurities, and as shown in Table I, they do not follow the trend observed for the relaxations. This indicates that the electronic structure plays an important role on the formation energies as will be discussed below. The results presented in Table I for PbSe are in reasonable agreement with Ga, In, and Tl in Pb sites of bulk PbTe,[22] where formation energies of 0.86, 0.48, and 0.66 eV have been obtained, respectively.

For a confined system, PbSe NW, the Pb sites are not equivalent. We can separate the NW in two different regions: (i) the core region where all Pb atoms are bound to six different Se atoms, as it is in the bulk (sites A to F of Fig. 1) and (ii) a

TABLE I. Formation ($E^f$) and relaxation ($E^{rel}$) energies (eV) for group III impurity doped PbSe NW and bulk. The NW label sites are indicated in Fig. 1.

| | Al | | Ga | | In | | Tl | |
|---|---|---|---|---|---|---|---|---|
| Site | $E^f$ | $E^{rel}$ | $E^f$ | $E^{rel}$ | $E^f$ | $E^{rel}$ | $E^f$ | $E^{rel}$ |
| A | 0.31 | 0.52 | 0.77 | 0.16 | 0.42 | 0.06 | 0.72 | 0.06 |
| B | 0.15 | 0.72 | 0.78 | 0.17 | 0.43 | 0.05 | 0.68 | 0.06 |
| C | 0.21 | 0.68 | 0.78 | 0.17 | 0.42 | 0.05 | 0.70 | 0.07 |
| D | −0.17 | 0.87 | 0.70 | 0.24 | 0.42 | 0.07 | 0.80 | 0.04 |
| E | −0.05 | 0.77 | 0.74 | 0.20 | 0.42 | 0.07 | 0.77 | 0.05 |
| F | 0.15 | 0.74 | 0.74 | 0.21 | 0.42 | 0.06 | 0.76 | 0.05 |
| G | −0.48 | 1.25 | 0.58 | 0.32 | 0.42 | 0.10 | 0.66 | 0.13 |
| H | −0.19 | 0.96 | 0.69 | 0.24 | 0.42 | 0.07 | 0.65 | 0.11 |
| I | −0.12 | 0.89 | 0.70 | 0.23 | 0.41 | 0.07 | 0.65 | 0.10 |
| J | −0.22 | 0.98 | 0.66 | 0.28 | 0.40 | 0.09 | 0.71 | 0.08 |
| Bulk | 0.56 | 0.40 | 0.85 | 0.07 | 0.40 | 0.03 | 0.75 | 0.02 |

surface region where the Pb atoms present a lower coordination number than the bulk one (sites G to J of Fig. 1). The most stable site for any group III impurity is on the surface. From Table I, we also observe that the impurity energetic stabilities are different from the NWs as compared to the same impurities in the bulk. For the energetically most stable impurity position, only for $In_{Pb}$, we obtain a similar formation energy in bulk and in NW. The most surprising result in Table I is the formation energy for $Al_{Pb}$, which is negative. We have to remember that we use Al metallic phase as the chemical potential, so we are in an Al-rich condition. It is interesting to note that the incorporation of Al impurity in NW presents a much lower formation energy than that of bulk PbSe, and it is the lowest among group III impurities in NW.

In order to understand the effects of the relaxations on the energetics, we compute the relaxation energy ($E^{\rm rel}$), which is the difference between the formation energies of the unrelaxed system and the relaxed one. In Table I, we observe that for an $Al_{Pb}$ defect, in the bulk we obtain $E^{\rm rel} = 0.40$ eV, while in the NW we obtain $E^{\rm rel} = 0.52$ and 1.25 eV when the Al impurity is in the core region (A site) and at the surface corner (G site), respectively. The analysis of the local geometry near the Al impurity shows that the Se nearest atoms relax to form a tetrahedral-like bond symmetry around the Al impurity. On the other hand, for Ga and In impurities, a different relaxation mechanism is observed. In bulk PbSe, $Ga_{Pb}$ impurities have the highest formation energy among the group III impurities studied, while $In_{Pb}$ impurities have the lowest one. This difference in the formation energies is related to the difference in the covalent radius between the impurity and the replaced Pb atom. In and Pb have a similar covalent radius, $\Delta R_c = 0.03$ Å, while Ga and Pb present a greater difference, $\Delta R_c = 0.21$ Å. The smaller covalent radius for Ga as compared to Pb introduces a stress around the impurity. In Table I, we can notice that the relaxation energies for both, bulk and NW, are greater for the Ga impurity as compared to In and Tl impurities, which have a covalent radius similar to Pb.

## IV. ELECTRONIC PROPERTIES

The calculated electronic structure for group III impurities in bulk PbSe reveals that, not only Al presents the unexpected $n$-type character, as observed experimentally by Zhang *et al.*,[25] but also In impurity induces $n$-type doping. It should be expected that group III elements, which have less electrons in the valence, would present $p$-type character when in Pb sites. However, our results show that Al and In impurities result in $n$-type doping, while Ga and Tl introduce acceptor levels. Androulakis *et al.*[21] also observed $n$-type character for Ga and In doped PbSe, but, while for In impurity our result is in agreement with theirs, for Ga impurity we obtain a $p$-like state, similarto the result obtained by Peng *et al.*[33]

In order to understand the unexpected semiconductor character of PbSe doped with group III impurities, we construct a two-level model.[26] An impurity ion with energy $\varepsilon_I$ in the Pb site interacts mostly with the valence band host Se-$p$ states, which have an energy $\varepsilon_H$. Within the two-level model, the interaction between $\varepsilon_I$ and $\varepsilon_H$ results in a bonding hyperdeep state ($E_{\rm HDS}$), and an antibonding deep defect state ($E_{\rm DDS}$), as schematically shown in Fig. 2. The splitting between these two

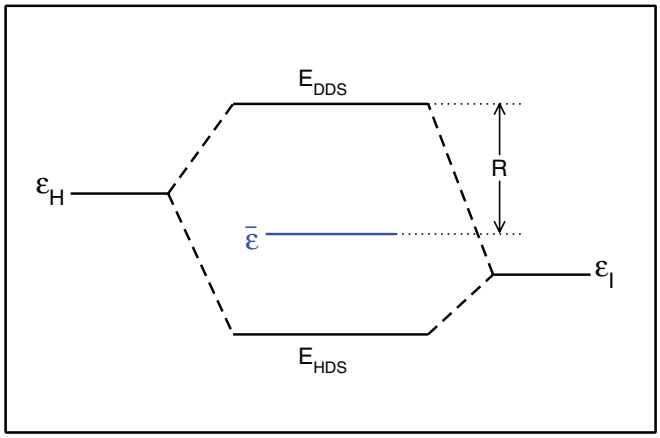


FIG. 2. (Color online) Schematic two-level model for a group III impurity in the Pb site of PbSe. $\varepsilon_I$ and $\varepsilon_H$ are the impurity ion $X$ and host Se states, respectively. $E_{\rm HDS}$ and $E_{\rm DDS}$ are the bonding and antibonding impurity states, respectively, resulting from the repulsion $R$ with respect to the $\bar{\varepsilon}$ average energy (see text).

energy levels can be expressed as

$$E_{\rm DDS,HDS} = \bar{\varepsilon} \pm \left(\Delta^2 + \epsilon_{IH}^2\right)^{1/2}, \qquad (2)$$

where $\bar{\varepsilon} = \frac{\varepsilon_I + \varepsilon_H}{2}$, $\Delta = \frac{\varepsilon_I - \varepsilon_H}{2}$, and $\epsilon_{IH}$ is the coupling matrix $\epsilon_{IH} = \langle I|\Delta V|H\rangle$, due to interaction between the impurity ion (I) and the host (H). The signs + and − denote $E_{\rm DDS}$ and $E_{\rm HDS}$, respectively. $\Delta$V is the difference in the potential when the Pb atom is substituted by an impurity (Al, Ga, In, or Tl). To obtain $\epsilon_{IH}$, we search in the DOS the $E_{\rm DDS}$ position, and

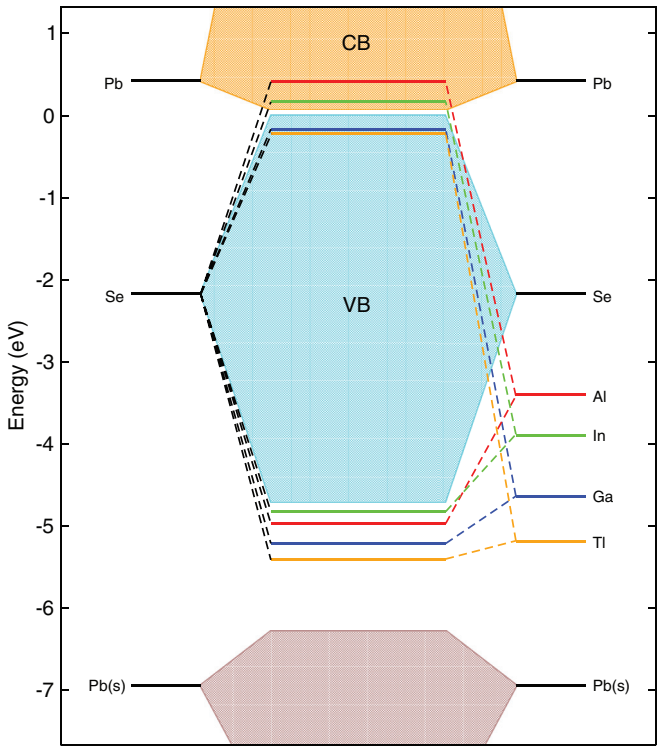


FIG. 3. (Color online) Schematic diagram of the calculated band structure and impurity levels $E_{\rm HDS}$ and $E_{\rm DDS}$ of group III doped bulk PbSe.

TABLE II. Two-level model parameters.

| | | | | $\epsilon_{IH}$ | | R | |
|---|---|---|---|---|---|---|---|
| Impurity | $\epsilon_I$ | $\bar{\epsilon}$ | $\Delta$ | bulk | NW | bulk | NW |
| Al | −4.73 | −4.12 | −0.62 | 3.14 | 3.33 | 3.37 | 3.39 |
| Ga | −5.96 | −4.73 | −1.23 | 2.99 | 3.32 | 3.23 | 3.54 |
| In | −5.22 | −4.36 | −0.86 | 3.08 | 3.97 | 3.20 | 3.09 |
| Tl | −6.51 | −5.01 | −1.51 | 3.11 | 3.94 | 3.46 | 3.30 |

then Eq. (2) is used to give the $\epsilon_{IH}$ value. We observe that the greater is the relaxation energy, the greater is $\epsilon_{IH}$, which rules the difference in energy between $E_{\mathrm{HDS}}$ and $E_{\mathrm{DDS}}$.

As the character $n$ or $p$ of a semiconductor is determined by the antibonding $E_{\mathrm{DDS}}$ state, we focus the discussion in this impurity state. The energy level position of the $E_{\mathrm{DDS}}$ is determined by the competition between $\Delta$ and $\epsilon_{IH}$ as well as by the absolute position of the isolated impurity energy ion level, $\varepsilon_I$.

The energy levels $\varepsilon_I$ and $\varepsilon_H$ have been determined as the $s$ and $p$ orbitals of the isolated atoms for the impurities and the Se atom, respectively. These energy levels have been computed by performing a DFT calculation with a supercell containing only one (impurity or host) atom and a common reference value. In this work, we use as reference the occupied level of a hydrogen molecule. Using the top of the valence band together with the reference $H_2$ molecule, the host $\varepsilon_H$ and the impurity $\varepsilon_I$ levels can be directly compared to the total (host+impurity) system. The parameters obtained from the DFT are summarized in Table II. Figure 3 shows the DFT energy splittings obtained from the projected density of states (PDOS), which can be directly compared to the two-level model described above. We observe that the level repulsion $R = (\Delta^2 + \epsilon_{IH}^2)^{1/2}$ is quite strong for all impurities, and it presents similar values for any impurity. So, there is a competition between $\Delta$ and $\epsilon_{IH}$, resulting in almost constant repulsion $R$. Al and In have isolated impurity levels, $\varepsilon_I$, at higher energy positions than Ga and Tl. Then, the $E_{\mathrm{DDS}}$ state for Al and In must be located in higher energy too, in accordance with our findings, where an $n$-type semiconductor is obtained for both impurities. Similar results have been observed for Ga, In, and Tl doped PbTe materials.[13,34] However, here, for PbSe we observe that there is no such trend when we go from Al down to Tl impurities of group III. Actually, Al and In present quite similar results, both are $n$-type dopants, while Ga and Tl form another class, which consists of $p$-type dopants. This trend can be understood by looking at the computed $\Delta$ and $\epsilon_{IH}$ parameters, which do not follow the periodic table of elements trend: we find $\Delta^{\mathrm{Al}} < \Delta^{\mathrm{In}} < \Delta^{\mathrm{Ga}} < \Delta^{\mathrm{Tl}}$, and inversely, $\epsilon_{IH}^{\mathrm{Al}} > \epsilon_{IH}^{\mathrm{In}} > \epsilon_{IH}^{\mathrm{Ga}} > \epsilon_{IH}^{\mathrm{Tl}}$. In this way, the classification in $n$- or $p$-type semiconductor

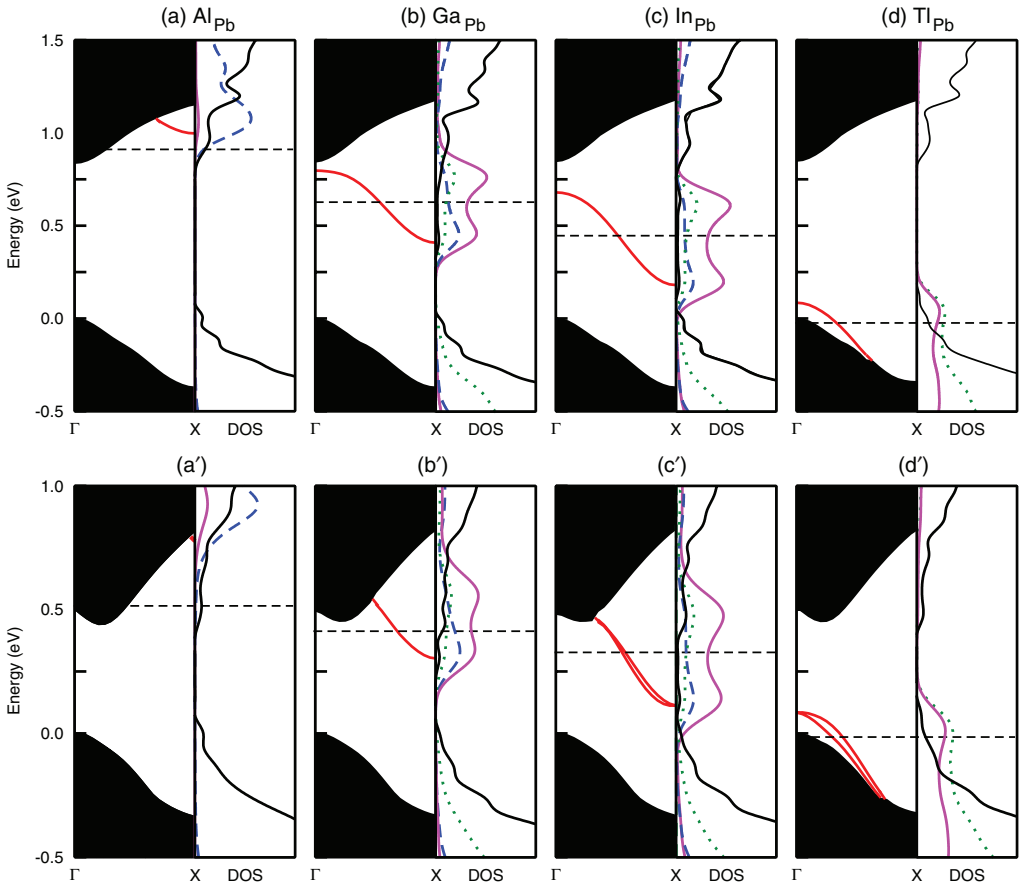


FIG. 4. (Color online) Calculated electronic band structure and DOS for PbSe NWs doped with group III impurities in the cation (Pb) site. From left to right, we have Al, Ga, In, and Tl. The upper part presents the results without the inclusion of SO interactions, while the botton presents the results with SO interactions. The horizontal dash-dotted lines represent the Fermi level, and the red lines are the impurity states. The PDOS for the impurities, Pb, and Se atoms are represented by solid (magenta), dashed (blue), and dotted (green) lines, respectively.

is determined by the impurity ion level $\varepsilon_I$, which raises or reduces the average $\bar{\varepsilon}$. In this way, we conclude that the unexpected $n$-type character for group III impurity doped PbSe is due to the strong $R$ repulsion observed in these systems, together with the absolute position of the impurity ion energy $\epsilon_I$.

The electronic properties of group III doped NWs, due to the quantum confinement effects, present a different behavior as compared to the same impurities in the bulk PbSe. In Fig. 4, we show the calculated electronic band structure and the density of states (DOS) for Al, Ga, In, and Tl in the most stable site of the NW. In the upper part, we present the results without SO, while in the bottom part, SO interaction has been included. We observe that the SO is important not only for the description of the conduction and valence bands, but also for the prediction of the correct position of the $E_{\mathrm{DDS}}$ levels. The impurity $E_{\mathrm{DDS}}$ levels are kept almost degenerate after turning on the SO interaction. For Al impurity, the $E_{\mathrm{DDS}}$ is resonant in the conduction band, pinning the Fermi level at the CBM, resulting in a $n$-type doping, similar to the result obtained for bulk PbSe. While Ga and In impurities in the bulk are acceptor and donor states, respectively, in the NW, these impurities create semioccupied deep donor states, but with large energy dispersions. Tl impurity introduces a shallow acceptor state, with the Fermi level at the VBM.

In order to better understand the interaction between the neighboring host Se atoms and group III impurities, we also search for the $E_{\mathrm{DDS}}$ and $E_{\mathrm{HDS}}$ impurity levels in the PbSe NW. As showed in Fig. 5, the Al impurity has the highest

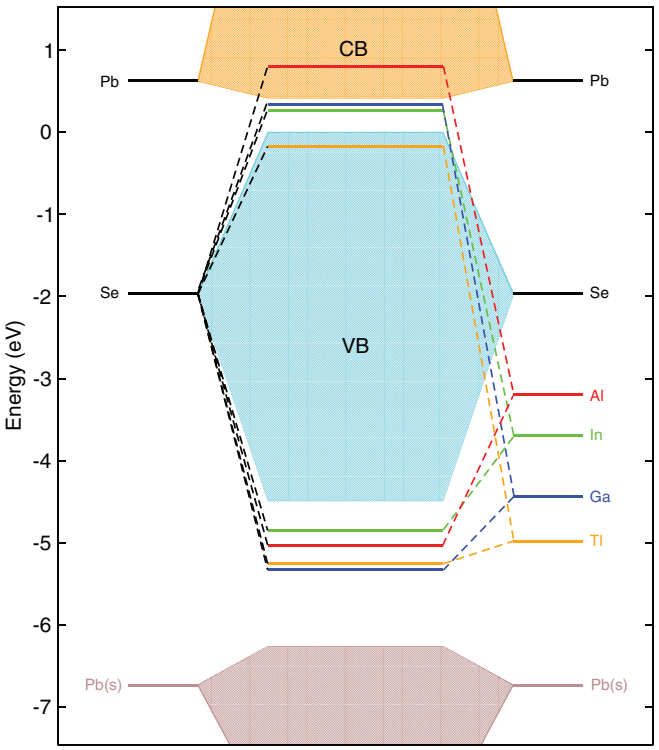


FIG. 5. (Color online) Schematic diagram of the calculated band structure and impurity levels $E_{\mathrm{HDS}}$ and $E_{\mathrm{DDS}}$ of group III doped PbSe NW.

energy $\varepsilon_I$, and the interaction between the impurity and the host system leads to an $E_{\mathrm{DDS}}$ state resonance in the conduction band. Although the impurity level $\varepsilon_I$ of the group III ions does not obey the atomic number order, the position of the $E_{\mathrm{DDS}}$ levels at the $\Gamma$ point recover the same order of the covalent radius variation. By comparing Figs. 5 and 3, we observe that the Ga impurity presents a $p$-type character in bulk PbSe, while in the NW it is a deep donor impurity, similar to the In impurity. Based on the two-level model described above, we observe that, although $\Delta$ is the same for the bulk and NW, since we have the same impurities, the main contribution for the position of the $E_{\mathrm{DDS}}$ level is the coupling interaction $\epsilon_{IH}$, which now has the following order: $\epsilon_{IH}^{\mathrm{Al}} > \epsilon_{IH}^{\mathrm{Ga}} > \epsilon_{IH}^{\mathrm{In}} > \epsilon_{IH}^{\mathrm{Tl}}$. The reason why Ga recovers the covalent radius order can be understood by looking at the relaxation and the formation energies in Table I. Ga doped bulk PbSe presents the highest formation energy, and almost no relaxation is observed (0.07 eV). On the other hand, for Ga doped PbSe NW, the relaxation increases significantly (0.32 eV), and the formation energy decreases from 0.84 to 0.58 eV.

Also it is interesting to analyze why for Al impurity the $E_{\mathrm{DDS}}$ level is so high inside the conduction band, even after considering the confinement effects in NW, which open the band gap. The answer is also related to the relaxations, similar to what is observed for the Ga impurity described above. By looking at the relaxation energies for the Al impurity in Table I, we observe that in the NW, the relaxations are stronger than in the bulk (1.25 eV as compared to 0.40 eV in the bulk). The stronger relaxations in the NWs result in a stronger coupling $\epsilon_{IH}$, which places the $E_{\mathrm{DDS}}$ resonant level in the conduction band.

Now we turn to the application of doped PbSe NW in TE systems. It has been shown that the Al doped bulk PbSe has a high figure of merit,[25] which was attributed to the presence of resonant states (Al derivatives) in the conduction band, increasing the local density of states. For PbSe NWs, we expect that not only Al, but also Ga and In impurities are potential systems for efficient TE devices. The character of the density of states around the Fermi level can be seen in Fig. 6, where we show the electronic charge density near the Fermi level for group III impurity doped PbSe NW. Figures 6(a)–6(c) show the highest occupied molecular orbital (HOMO) for $\mathrm{Al_{Pb}}$, $\mathrm{Ga_{Pb}}$, and $\mathrm{In_{Pb}}$, respectively, at the $X$ point. Figure 6(d) shows the lowest unoccupied molecular orbital (LUMO) for $\mathrm{Tl_{Pb}}$ impurity at the $\Gamma$ point. It is interesting to note that the HOMO at the $X$ point of $\mathrm{Al_{Pb}}$ is mostly localized on Pb atoms, which is the main contribution for the CBM. So the Al impurity will increase the density of states at the CB, which may increase the figure of merit. On the other hand, the HOMOs for $\mathrm{In_{Pb}}$ and $\mathrm{Ga_{Pb}}$ have contributions from Se and Pb atoms, placing the DDS between the CBM and VBM. We also notice that the LUMO of the $\mathrm{Tl_{Pb}}$ is strongly localized on the surface of the NW, mainly in two Se atoms nearest neighbors of the Tl impurity, aligned parallel to the NW axis. So, Tl impurity induces a typically $p$-type doping. It is worth to point out that the electronic charge density for the defect states (see Fig. 6) is in accordance with the PDOS shown in Fig. 4, where $p$- and $n$-type impurities present a greater contribution for the defect states coming from the Pb and Se atoms, respectively.

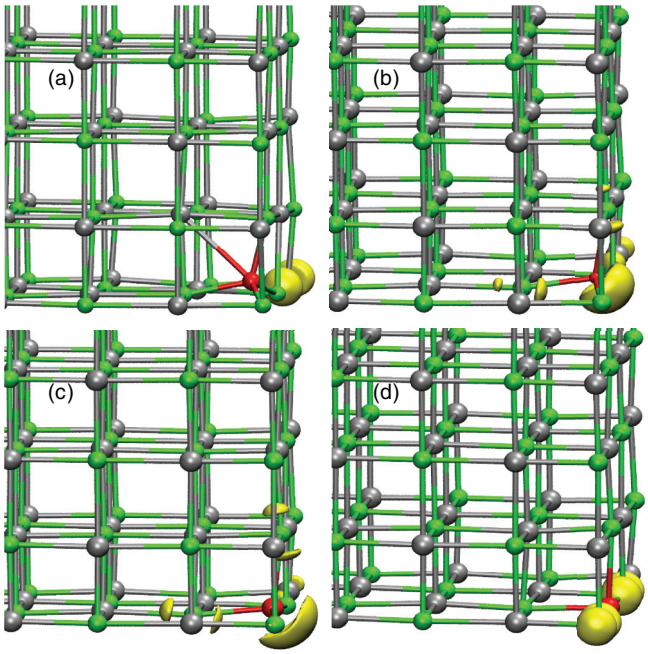


FIG. 6. (Color online) Calculated electronic charge density; (a)–(c) of HOMOs at the $X$ point for $Al_{Pb}$, $Ga_{Pb}$, and $In_{Pb}$, respectively, and (d) LUMO at the $\Gamma$ point for $Tl_{Pb}$.

## V. DISCUSSIONS AND CONCLUSIONS

From the results described above, we observe that different impurities of group III exhibit different electronic properties in bulk PbSe. We also notice that the same impurity can show different electronic properties in bulk as compared to NW. These results can be understood by using a two-level model, where the interaction between the impurity levels an the host PbSe are considered. The difference in energy between the impurity levels $E_{HDS}$ and $E_{DDS}$ shown in Figs. 3 and 5, is an effect of how differently the impurity levels and the crystalline field interact in the bulk and in a confined system. For the bulk, we observe that group III impurities are shallow donors ($Al_{Pb}$ and $In_{Pb}$), or acceptor ($Ga_{Pb}$ and $Tl_{Pb}$) impurities. For the NW, we observe similar trends for $Al_{Pb}$ and $Tl_{Pb}$, however, owing to the quantum confinement effects (the band gap opens) and the different coordination for the impurity in the surface of the NW, $Ga_{Pb}$ and $In_{Pb}$ introduce a defective electronic level within the NW band gap.

The two-level model based on the interaction between the impurity states and the host crystalline field, together with the computed DFT *ab initio* parameters (mainly the PDOS), explains the unexpected transition from $n$- to $p$-type character of group III impurity doped PbSe when we go down from Al to Tl. We also observe that this model is still working to explain the differences in the electronic properties for the same impurity in the bulk and in the NW but here the effects of the relaxations must be used to understand the trend of group III doped PbSe NWs.

The calculated formation energies of group III impurity doped bulk PbSe and PbTe are similar to each other (see Table I and Ref. 22), and here we show that they are greater than the same impurities in NWs. So, for a quantum confined system, as the PbSe NW, the incorporation of group III impurities should be easier, since the formation energies are lower. Actually, our first-principles results show that $Al_{Pb}$ on the surface of a NW is an exothermic process and, most interesting, the electronic properties for Al doped PbSe NW are quite similar to that of bulk PbSe, which has been showed to present a high figure of merit for TE applications.[25] Group III impurities segregate to the surface of the NW, where a lower formation energy is observed for $Al_{Pb}$, $Ga_{Pb}$, and $Tl_{Pb}$ as compared to the bulk system. The lower formation energy in the surface as compared to the core is associate with a higher relaxation energy, decreasing the strain. For $In_{Pb}$, almost the same formation energy has been obtained in all sites along the NW diameter, and these formation energies are very similar to that obtained for the bulk one.

It has been already shown that confined systems like Si NWs,[10] present better TE performance than their bulk counterparts. The improvement in the TE efficiency for a low-dimensional system is attributed to the decrease in the thermal conductivity, which is inversely proportional to the NW diameter.[11] In addition, we show that impurities can improve the TE properties by introducing distortions in the density of states around the Fermi level. Our first-principles calculations show that doped PbSe NW can be a better material for TE applications than the precursor bulk PbSe.

## ACKNOWLEDGMENTS

We want to thanks the CENAPAD-Campinas for the computer facilities and the Brazilian agencies CNPq, CAPES, FAPEMIG, and FAPERGS for the financial support.

*rbaierle@smail.ufsm.br

[1] J. John and H. Zogg, J. Appl. Phys. **85**, 3364 (1989).
[2] J. P. Heremans, C. M. Thrush, and D. T. Morelli, Phys. Rev. B **70**, 115334 (2004).
[3] Y. Gelbstein, Z. Dashevsky, and M. P. Dariel, J. Appl. Phys. **104**, 033702 (2008).
[4] S. Nadj-Perge, S. M. Frolov, E. P. A. M. Bakkers, and L. P. Kouwenhoven, Nature (London) **468**, 1084 (2010).
[5] S. Jin, H. Wu, and T. Xu, J. Appl. Phys. Lett. **95**, 132105 (2009).
[6] M. Rahin, M. Arnold, F. Felder, K. Behfar, and H. Zogg, Appl. Phys. Lett. **91**, 151102 (2007).
[7] M. Bobert, T. Fronherz, J. Roither, G. Pillwein, G. Spingholz, and W. Heiss, Appl. Phys. Lett. **88**, 041105 (2006).
[8] K. Hummer, A. Grüneis, and G. Kresse, Phys. Rev. B **75**, 195211 (2007).
[9] E. O. Wrasse, R. J. Baierle, T. M. Schmidt, and A. Fazzio, Phys. Rev. B **84**, 245324 (2011).
[10] A. I. Boukai, Y. Bunimovich, J. T.- Kheli, J.-K. Yu, A. Goddard III, and J. R. Heath, Nature (London) **451**, 168 (2008).

[11]G. Pernot, M. Stoffel, I. Savic, F. Pezzoli, P. Chen, G. Savelli, A. Jacquot, J. Schumann, U. Denker, I. Mönch, C. Deneke, O. G. Schmidt, J. M. Rampnoux, S. Wang, M. Plissonnier, A. Rastelli, S. Dilhaire, and N. Mingo, Nat. Mater. **9**, 491 (2010).

[12]R. Chen, A. I. Hochbaum, P. Murphy, J. Moore, P. Yang, and A. Majumdar, Phys. Rev. Lett. **101**, 105501 (2008).

[13]S. Ahmad, K. Hoang, and S. D. Mahanti, Phys. Rev. Lett. **96**, 056403 (2006).

[14]K. Hoang and S. D. Mahanti, Phys. Rev. B **78**, 085111 (2008).

[15]J. P. Heremans, V. Jovovic, E. S. Toberer, A. Saramat, K. Kurosaki, A. Charoenphakdee, S. Yamanaka, and G. J. Snyder, Science **321**, 554 (2008).

[16]Y. Pei, X. Shei, A. LaLonde, H. Wang, L. Chen, and G. J. Snyder, Nature (London) **473**, 66 (2011).

[17]K. Biswas, J. Q. he, Q. C. Zhang, G. Y. Wang, C. Uher, V. P. Dravid, and M. Q. Kanatzidis, Nat. Chem. **3**, 160 (2011).

[18]P. F. R. Poudeu, J. D'Angelo, A. D. Downey, J. L. Short, T. P. Hogan, and M. G. Konatzidis, Angew. Chem. Int. Ed. **45**, 3835 (2006).

[19]K. F. Hsu, S. Loo, F. Guo, W. Chen, J. S. Dyck, C. Uher, T. Hogan, E. K. Polichroniadis, and M. G. Kanatzidis, Science **303**, 818 (2004).

[20]J. Androulakis, C. H. Lin, H. J. Kong, C. Uher, C. I. Wu, T. Hogan, B. A. Cook, T. Caillat, K. M. Paraskevoupolus, and M. G. Kanatzidis, J. Am. Chem. Soc. **129**, 9780 (2007).

[21]J. Androulakis, Y. Lee, I. Todorov, D.-Y. Chung, and M. Kanatzidis, Phys. Rev. B **83**, 195209 (2011).

[22]K. Hoang, S. D. Mahanti, and P. Jena, Phys. Rev. B **76**, 115432 (2007).

[23]The efficiency of a TE material is measured by its figure of merit ($ZT$), the dimensionless $ZT$ is defined as $ZT = \frac{S^2\sigma}{\kappa}$, where $S$ is the Seebeck coeficient, $\sigma$ is the electrical conductivity, and $\kappa$ is the thermal conductivity. $T$ is the absolute temperature.

[24]K. Lischka, Appl. Phys. A **29**, 177 (1982).

[25]Q. Zhang, H. Wang, W. Liu, H. Wang, B. Yu, Q. Zhang, Z. Tian, G. Ni, S. Lee, K. Esfarjani, G. Chen, and Z. Ren, Energy Environ. Sci. **5**, 5246 (2012).

[26]M. J. Caldas, A. Fazzio, and A. Zunger, Appl. Phys. Lett. **45**, 671 (1984).

[27]J. P. Perdew, K. Burke, and M. Ernzerhof, Phys. Rev. Lett. **77**, 3865 (1996).

[28]G. Kresse and J. Furthmüller, Phys. Rev. B **54**, 11169 (1996).

[29]G. Kresse and J. Furthmüller, Comput. Mater. Sci. **6**, 15 (1996).

[30]G. Kresse and D. Joubert, Phys. Rev. B **59**, 1758 (1999).

[31]C. E. Ekuma, D. J. Singh, J. Moreno, and M. Jarrell, Phys. Rev. B **85**, 085205 (2012).

[32]H. J. Monkhorst and J. D. Pack, Phys. Rev. B **13**, 5188 (1976).

[33]H. Peng, J.-H. Song, M. G. Kanatzidis, and A. J. Freeman, Phys. Rev. B **84**, 125207 (2011).

[34]C. M. Jaworski, B. Wiendlocha, V. Jovovic, and J. P. Heremans, Energy, Environ. Sci. **4**, 4155 (2011).